

Mean Field Dynamics of Graphs II: Assessing the Risk for the Development of Phase Transitions in Empirical Data

Jolanda J. Kossakowski,^{1,*} Marijke C. M. Gordijn,² Harriëtte Riese,³ and Lourens J. Waldorp¹

¹*Department of Psychology
University of Amsterdam
Nieuwe Achtergracht 129-B
1018 XE Amsterdam
The Netherlands*

²*Department of Chronobiology
GeLifes, University of Groningen
Groningen, The Netherlands*

³*Interdisciplinary Center Psychopathology and Emotion regulation
Department of Psychiatry
University Medical Center Groningen
University of Groningen, Groningen, The Netherlands*
(Dated: December 1, 2023)

Psychological disorders like major depressive disorder can be seen as complex dynamical systems. By looking at symptom activation patterns, we can investigate the dynamic behaviour of individuals to see whether or not they are at risk for sudden changes (phase transitions). Here, we show how a mean field approximation is used to reduce a dynamic multidimensional system to one-dimensional system to analyse the dynamics. Using maximum likelihood estimation, we can estimate the parameter of interest which, in combination with a bifurcation diagram, reflects the risk that someone has for experiencing a transition. After validating the proposed method with simulated data, we apply this method to three empirical examples, where we validate our method using data that contains a transition, and where we show its use in a clinical and general sample. Results show an increased risk for a transition when the transition actually occurred, and that members of both a clinical and general sample did not show an increased risk for a transition. We conclude that the mean field approximation has great potential in assessing the risk for a transition; with some expansions and it could, in the future, aid clinical therapists in the treatment of depressed patients.

PACS numbers: 64.60.aq, 05.45.-a

Keywords: cellular automata, discrete dynamical system, nonlinear dynamics, bifurcation, psychopathology

I. INTRODUCTION

Major depressive disorder (MDD) is unfortunately not that uncommon: around 350 million people around the globe suffer from MDD [1]. When recovered from MDD, people have a 50% risk of relapsing [2]. With so many suffering from MDD comes an even larger amount of costs of treatment, societal costs, and intangible costs like stereotyping. While many studies have been conducted in the treatment of MDD, it is known that prevention is better than curing, and it is therefore essential that we gain more insight into the development and onset of MDD. In the companion paper [3], Waldorp and Kossakowski showed, both analytically and by means of an extensive simulation study, how *complex dynamical systems* can be reduced to one-dimensional discrete time dynamical systems. The goal of this paper is to illustrate the potential of this method by applying it to empirical data.

Psychological disorders like MDD can be seen as a complex dynamical system: symptoms of MDD, like loss of energy of feelings of worthlessness, can be seen as nodes in a network that interact, and thereby influence, itself and other symptoms of MDD [4]. This *system* of interacting symptoms

may change over time, making the system *dynamic* [5]: the influence of sleep deprivation on feelings of worthlessness may grow over time, as an individual is feeling more and more depressed. We can measure these changes by means of the *Experience Sampling Method* (ESM) [6], where individual daily life experiences can be measured several times a day for an extended period of time [7]. See Telford et al. [8] and aan het Rot et al. [9] for more information on ESM. In the development of MDD, the system surpasses a critical point [10], and a discontinuous transition is made; a transition from a stable, healthy phase to a stable, depressed phase. These sudden jumps, called *phase transitions* or critical transitions [11], are central to complex dynamical systems, and are subject of the risk assessment that we will undertake in the present paper.

While phase transitions occur suddenly, complex dynamical systems leave ‘breadcrumbs’ behind that hint towards a phase transition. These breadcrumbs are called *early-warning signals* and occur before the phase transition, and after *critical slowing down* [10]. Every individual has a so-called average mood state: when you have a bad day, you may feel worse than average, but your mood will always return to that average mood state. When you are developing MDD, you are slowly deviating from your personal average mood state. As you are getting closer and closer to the tipping point at which a phase transition occurs, it will become harder and harder to return to that average mood state. In other words, your dynamic system

* Corresponding author: J.J.Kossakowski@uva.nl

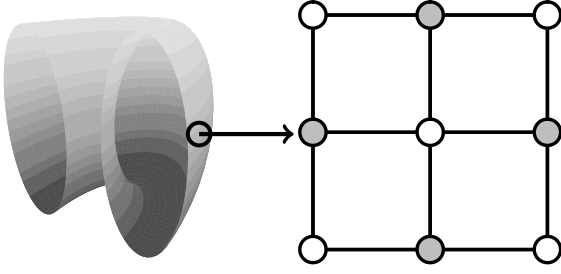


Figure 1: Visualization of half a torus (left figure), and a close-up that shows the grid structure (right figure).

of MDD ‘slows down’ so that it is more difficult to return to the average mood state. Recently, it has been shown that critical slowing down actually occurs, prior to the phase transition [12, 13].

By looking at the proportion of ‘active’ symptoms at individual measurements, and by assuming that symptoms behave in the same way to a certain extent, we can investigate the dynamic behaviour of the system using a *mean field approximation*. By showing three empirical examples, we demonstrate how our method works on different types of time-series data. This paper is set up as follows: first, we explain the mean field approximation and the proposed method. Then we present a validation study to show how well the proposed method works. Lastly, we apply the proposed method on three different types of time-series data to show how the proposed method works in practice.

A cellular automaton (CA) is a dynamical system where nodes are arranged in a fixed and finite grid, and where connected nodes determine the state of a node at each subsequent time point [14, 15]. A grid is a graph $G_{\text{grid}}(n, \Gamma)$ with n nodes in the set $V = \{1, 2, \dots, n\}$ where each node x is connected to nodes in the neighbourhood $\Gamma = \{y \in V : y \text{ is connected to } x\}$. To ensure all nodes have exactly the same number of neighbours, we invoke the boundary condition such that a node at the boundary is connected to a node on the opposite end, making it a torus. An example of such a grid is shown in Figure 1, where the middle node is directly connected to four other nodes (a node’s neighbourhood), marked in grey [16]. We consider elementary CAs where each node can be in either of two states: ‘active’ (coded by 1) or ‘inactive’ (coded by 0). In a CA a deterministic, local update rule ϕ determines the state of each node based on which nodes are active in the neighbourhood of x . An example of this is the majority rule, where each node becomes 1 whenever more than half of the neighbours of x are active, and 0 otherwise. Although many other update rules are possible, we will focus on this particular rule in the present paper. Repeated application of the update rule ϕ results in a vector of 0s and 1s called an orbit: At any time point t the orbit $\phi^t(x) = \phi(\phi \cdots \phi(x))$, such that the same local rule is applied t times.

In a probabilistic cellular automaton (PCA), a probability is introduced to model uncertainty, based on the number of active neighbours. In our application to psychopathology,

this uncertainty is required because we cannot predict the behaviour of the symptoms in our network exactly, and because we know that exogenous events influence these symptoms which we cannot measure. The probability $0 \leq p \leq 1$ determines whether or not a node becomes active at time point $t + 1$. The majority rule with the probabilistic update used in this paper is

$$\xi_{|\Gamma|}(r) = \begin{cases} p & \text{if } r \leq |\Gamma|/2 \\ 1 - p & \text{if } r > |\Gamma|/2 \end{cases} \quad (1)$$

where $|\Gamma|$ is the size of the neighbourhood and r the number of active neighbours. Because $\xi_{|\Gamma|}$ is dependent on the behaviour of the majority of a node’s neighbourhood, this update rule is also called the *majority rule*. In this PCA each node $x \in V$ is then updated according to the majority rule; all nodes are updated simultaneously (synchronous updating). The result for each node is a sequence of 0s and 1s. For all $n = |V|$ nodes we have the orbits $(\phi^t(x), t \geq 0)$, which are vectors of length T for the total duration. We average all nodes at each time point t , $\rho_t = \sum_{x \in V} \phi^t(x)/n$, which we call the *density*. In sum, in a PCA nodes can switch between being active or inactive; these switches are determined by means of a probability that in turn depends on a node’s active neighbourhood.

II. MEAN FIELD APPROXIMATION

The PCA described above is a dynamical system with many components (nodes) that switch between active and inactive states. To infer from such a large-scale system some characteristics of what the system will do in the long run can be rather difficult [17]. Here we use the uniformity property of the graphs that allow us to reduce the n -dimensional system to a one-dimensional system. In the grid it is easily seen that each node is similar to any other node since each node has the same number of neighbours, and becomes active or inactive in the same way by means of the majority rule that is based on the number of active neighbours. This allows us to simplify a PCA to a single discrete time dynamical system, as in Kozma et al. [18] and Balister, Bollobás and Kozma [19]. Here we explain in general terms how we obtain the mean field approximation, but for more details, see our companion paper in this issue of Physical Review E [3].

In a *mean field approximation*, we assume that the properties of interest are uniform over the graph, which means that each node in the graph behaves in a similar manner and that each node has the same neighbourhood size $|\Gamma|$. Therefore, equation (1) only depends on the number of active nodes in Γ , denoted by r . To obtain the probability of a node being active given the majority rule in (1), we need to know the probability of a neighbourhood having r active nodes. The mean field assumption, implying uniform neighbourhoods over the entire graph G_{grid} , suggests we can reduce the graph to one equation that explains the behaviour for all nodes. Because all nodes are similar with respect to their neighbours, we can model the probability of a node being active at time point $t + 1$ by a random draw of any of the nodes in the graph at time point t [18, 19]. We therefore obtain a binomial probability, wherein

the number of active nodes in the neighbourhood Γ is considered, and has $|\Gamma|$ Bernoulli trials that each have a success probability ρ_t , the proportion of active nodes. The majority rule determines the size of the neighbourhood to be evaluated since we obtain p for all neighbourhood sizes with active nodes up until $\lfloor \Gamma/2 \rfloor$, and $1 - p$ otherwise. Let

$$\pi_{|\Gamma|/2}(\rho_t) = \sum_{r=0}^{\lfloor \Gamma/2 \rfloor} \binom{|\Gamma|}{r} \rho_t^r (1 - \rho_t)^{|\Gamma|-r} \quad (2)$$

where $\lfloor \Gamma \rfloor$ is the integer part of Γ . Then, as Balister et al. [19] showed and restated in Waldorp and Kossakowski [3], we obtain the probability of a node being active given the majority rule (1)

$$p_{\text{grid}}(\rho_t) = p\pi_{|\Gamma|/2}(\rho_t) + (1 - p)(1 - \pi_{|\Gamma|/2}(\rho_t)) \quad (3)$$

Plugging in different values for p , ranging from 0.1 to 0.5, we obtain a *bifurcation diagram*, of which an example is shown in Figure 2. In a bifurcation diagram the repeated application of p_{grid} is applied to updated values of ρ_t such that the last section of the orbit is displayed [20]. Such diagrams show what kind of behaviour can be expected to be generated by the process. Here we see that there are two kinds of situations: (a) a stable situation, where irrespective of the starting point, the process ends up at that stable fixed point, and (b) a bistable situation where the process could suddenly switch between states (phase transition). The parameter value p at which the process changes from a stable to a bistable situation is called the critical point. In Figure 2 the critical value lies at $p \approx 0.23$; the parameter area $0.1 \leq p \leq 0.23$ is bimodal where phase transitions can occur, whereas the parameter area $0.23 < p < 0.5$ represents a unimodal area where the mean field is stable.

The probability for the mean field in (3) is designed for a torus with a fixed neighbourhood size $|\Gamma|$. In the context of psychology and psychopathology, it is hard to come up with a graph representing the interactions between symptoms, that would take the form of a grid (torus). We therefore also looked at the mean field approximation for a *random graph* and a *small-world graph*.

A random graph $G_{\text{rg}}(n, p_e)$ is a graph structure with n nodes and a (constant) probability p_e for an edge to be present in the graph [21, 22]. In the mean field approximation of a random graph, the neighbourhood size Γ is a random variable that is maximally $n - 1$. Let $v = \lfloor p_e(n - 1) \rfloor$ be the integer part of the expected number of neighbours with probability of an edge p_e . The probability for a node to become active given the graph's density at time point t and the edge probability then becomes (see companion paper in this issue)

$$p_{\text{grid}}^v(\rho_t) = p\pi_v(\rho_t) + (1 - p)(1 - \pi_v(\rho_t)) \quad (4)$$

The difference with the probability on the grid is in the size of the neighbourhood, here for the random graph G_{rg} it is v and in the grid G_{grid} it is $\lfloor \Gamma/2 \rfloor$, where $|\Gamma|$ often is 5 in a two-dimensional grid (4 neighbours and the node itself at the previous time point). It can be shown that this approximation for the probability of a node being active is accurate (see companion paper in this issue).

A small-world graph is a graph where, compared to a random graph, the average clustering is high and the average path length is low [23]. A modified version of the small world graph is the Newman-Watts (NW) small-world graph [24]. In the NW small-world $G_{\text{sw}}(n, \Gamma, p_w)$ the n nodes each have a neighbourhood Γ as in the grid and edges are added to the graph following a (constant) wiring probability p_w [24]. We can then split up the probability in a part associated with the grid and a part associated with the random graph. The part for the grid is adjusted such that it corresponds to no other edges being present, i.e., we obtain $p_{\text{grid}}^{\text{sw}} = p_{\text{grid}}(1 - p_w)^{n-|\Gamma|}$. Then for the random part we obtain exactly those possible edges that could be included in the neighbourhood out of the remaining $n - |\Gamma|$ nodes that are possibly active, i.e., $p_{\text{grid}, \Gamma}^v$, which denotes the probability as in (4) but starting at $|\Gamma| + 1$. Then the probability for a node to become active given the graph's density at time point t and the wiring probability in the small-world graph G_{sw} is

$$p_{\text{sw}}(\rho_t) = \frac{|\Gamma|}{n} p_{\text{grid}}(1 - p_w)^{n-|\Gamma|} + \frac{n - |\Gamma|}{n} p_{\text{grid}, \Gamma}^v \quad (5)$$

The small-world probability is therefore a combination of the probability on the grid and on a random graph, proportionately weighted. In sum, a mean field approximation reduces a graph to a single equation, which we then can use to explain the graph's behaviour at different values for p .

III. ESTIMATION OF PROBABILITY p AND GRAPH PARAMETERS

Our objective is to determine from time series of the density of a graph obtained from real data, an estimate of whether or not this person is at risk of suddenly transitions to a different state, perhaps depression. One way of obtaining such a risk assessment is to determine where in a bifurcation diagram a person is located; is this in the stable area, where no transition can occur, or is it in the bistable area where a transition can occur. In order to do this, we need to estimate the parameter p of the majority rule. Here we use maximum likelihood (ML) to obtain an estimate of p [25].

We recognise in the PCA (see also the companion paper in this issue) that we can relatively easily find the transition probability to go from u to v active nodes by the fact that we have for each of the graphs G_{grid} , G_{rg} , and G_{sw} a binomial process with a probability of success particular to each type of graph. It follows that transition probability that the number of active nodes $n\rho_{t+1} = v$ given that at t is $n\rho_t = u$ in the graph G_{grid} is

$$\mathbb{P}(n\rho_{t+1} = v \mid n\rho_t = u) = \binom{n}{r} p_{\text{grid}}(u/n)^r (1 - p_{\text{grid}}(u/n))^{n-r} \quad (6)$$

The transition probabilities for the random graph G_{rg} and the small-world graph G_{sw} are similar except that we change the probability of success to p_{rg} or p_{sw} , respectively.

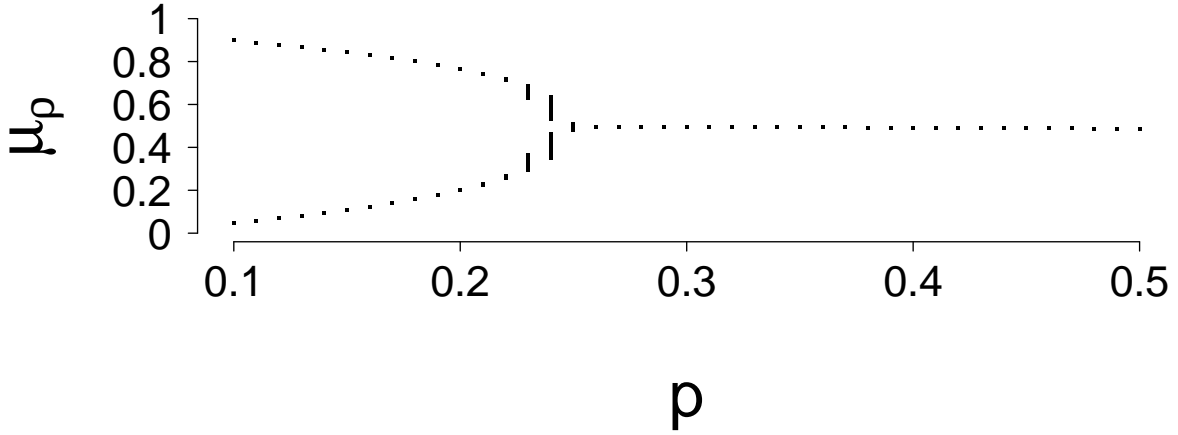


Figure 2: A bifurcation diagram for the mean field in the graph G_{grid} . μ_p = the network's density. p = the probability used in equation (3).

If we take a closer look at equations (2) and (3), it can be noticed that all parameters are known prior to the analysis, with the exception of the probability parameter p . To obtain the probability parameter p , we can estimate it from the data using ML estimation. We then obtain the maximum of the log-likelihood for the majority rule parameter p . We write the transition probability in going from state u to state v (number of active nodes) in (6) from t to $t + 1$ as $\mathbb{P}(np_{t+1} = v \mid np_t = u) = p_{u_t v_{t+1}}$. The log of the joint probability function (log-likelihood) for the number of active nodes is then

$$\log \mathbb{P}(np_t, t \geq 0) = \sum_{t=0}^{T-1} \log p_{u_t v_{t+1}} \quad (7)$$

We do not assume stationarity and so cannot simplify the log-likelihood to terms consisting only of the states and not on time [26]. We then maximise the log-likelihood function in (7) with respect to p to obtain its estimate from an empirical time series, making it possible to place that person on the bifurcation diagram and assess the risk of possible switching.

In both the random and small-world graph we have additional graph parameters: in the random graph we have the probability of an edge p_e , and in the small-world graph we have the probability of wiring p_w . Estimating p_e is not strictly necessary since we have an estimate simply by counting the number of present edges and dividing by the number of possible edges. But for the wiring probability p_w in the small-world graph, it may be useful as there is no method yet to determine this. Such an estimate is obtained by maximising the log-likelihood with respect to p_w . Obviously, for small graphs this will be difficult since we work with the NW small-world, implying that a grid structure is in place and some additional edges are randomly added.

IV. VALIDATION OF PROBABILITY p AND GRAPH PARAMETERS

We used simulated data from Waldorp & Kossakowski [3] to validate the estimation of p and the graph parameters p_e and p_w . These data were simulated in order to evaluate the accuracy of the mean field approximation. We varied the size of the network $n \in \{16, 25, 49, 100\}$, the number of time points $T \in \{50, 100, 500\}$, and the probability $p \in \{0.1, 0.2, 0.3, 0.4, 0.5\}$. We also varied $p_e \in \{0.1, 0.2, 0.3, 0.4, 0.5\}$ and $p_w \in \{0.1, 0.2, 0.3, 0.4, 0.5\}$. For each of the 100 simulation runs, we used the $t \times n$ set of active and inactive nodes to optimize p and the graph parameters. All simulated data, figures, and the used R-code are publicly available at the OSF [27]. For clarity of presentation, figures are only presented for $T = 500$, as results for $T = 50$ and $T = 100$ are similar in nature.

For each simulation run, we calculated the absolute difference between the value p , under which the data were simulated, and \hat{p} , which we estimated from the data. We denoted this difference by Δ_p , after which the mean absolute difference ($\bar{\Delta}_p$) is determined for each condition. The lower this value, the closer the estimate \hat{p} is to the original value p . The same procedure was performed to determine the accuracy for graph parameters p_e ($\bar{\Delta}_{p_e}$) and p_w ($\bar{\Delta}_{p_w}$). Figure 3 shows a 3D representation of the mean absolute difference between ($\bar{\Delta}_p$) the simulated parameters p , and \hat{p} for selected configurations. It can be seen that the mean absolute difference for p is low for all different network structures. The only exception to this is shown in the middle column of Figure 3, where $\bar{\Delta}_p$ is somewhat higher at low values for p , and decreases as p increases, similar to the results found in Figure 8 of the companion paper

in this issue.

The same conclusion cannot be made for graph parameters p_e and p_w , as seen in Figure 4. For a random graph, $\bar{\Delta}_{p_e}$ is high when p_e is low, and decreases. This shows that graph parameter \hat{p}_e is most accurate when p_e is high. A possible explanation for this finding could be found in the connectedness of random graphs. when p_e is small, the probability that not all nodes are connected increases, resulting in isolated nodes. When we look at the minimum probability p_e , such that the graph is connected for different N , we see that p_e must be at least 0.46 when the network size is 16, 0.31 when the network size is 25, 0.17 when the network size is 49 and 0.09 when the network size is 100. Thus, as p_e increases, the probability for the network to be connected increases, and as a result of this, $\bar{\Delta}_{p_e}$ decreases. The reverse is true for a small world graph, where $\bar{\Delta}_{p_w}$ is high when p_w is high and p is low, and that it decreases when p_w also decreases. Here, high values for p_w indicate large deviations from the grid (torus) structure, and thereby the approximation becomes less accurate. This shows that graph parameter \hat{p}_w is most accurate when p_w is low and when p is high.

V. APPLICATION TO EMPIRICAL TIME-SERIES DATA

In the following section, we will demonstrate how the probability of a symptom to be active p and the probability for an edge to be rewired p_w can be estimated from empirical data. Both random graphs and small world graphs are found in real-world networks, like social networks [28, 29], co-author networks [30], and psychopathological symptom networks [31, 32]. As there is currently no valid test to distinguish a random graph from a small world graph, we assume all graphs to be a random graph in the following empirical examples.

In the following three sections, we will show three empirical examples and demonstrate how the proposed method works on each of these datasets. By showing the application of our proposed method on three different kinds of data, we aim to show how our proposed method works for different participants, and different types of data. The first is a dataset of a single participant that contains almost 1500 measurements that were collected in a period of 239 days [13, 33]. The second is a dataset of patients who were admitted as patients on closed, psychiatric ward of an academic hospital [34, 35]. Lastly, the third example is a dataset of healthy participants who were originally recruited in a nation-wide study [36].

The data in these examples are time-series data. When collecting these types of data, participants are asked to complete a questionnaire several times a day. These questionnaires often contain items regarding a participant's current mood state, but can also hold items regarding a participant's physical condition, for example. In the first example, the participant's waking hours were divided into ten intervals. In each of these intervals, the participant received a 'beep' and was asked to complete the questionnaire at that specific point in time. For the other two examples, the time of the beeps were a priori set. These beeps, in turn, correspond to the time points in

time-series data. For example, when a participant completed twenty questionnaires, the data contains $t = 20$ time points.

Each empirical example has a similar set-up. We first start with removing items that were left unanswered for all time points, since these items cannot transport any information through the network and thus cannot be used to assess the risk for a critical transition. Items that were not answered (missing) were replaced with the answer at the previous time point $t - 1$, hereby replacing any missing data that may be present in the data. For each item, we determined how many times each response option (either 0 or 1) was recorded. In the case that one of the two response categories was observed less than four times, the item will be removed from the entire analysis. The data that is left after this process is then used to estimate p and p_w .

After these data cleaning steps, we estimate the network structure using the R-package IsingFit version 0.3.1 [37, 38]. IsingFit obtains edge coefficients by means of ℓ_1 -penalized nodewise regressions. As shown in Ravikumar, Wainwright and Lafferte [39], this procedure results in a sparse network with a high probability of correct zero and non-zero estimates of the edge coefficients. The higher the ℓ_1 -penalty (denoted by γ), the stronger the penalty and the more edges that are set to zero. The ℓ_1 -penalty needs to be chosen carefully: is the penalty too high, we may end up with a network without any edges. If the penalty is too low, we may end up with a network that is neither sparse nor informative. In order to select the most appropriate ℓ_1 -penalty, we test for values in the range $\{0, 1.5\}$ at which value the fewest number of edges are being pushed to zero. We then select this value to estimate the network.

When the network structure is determined, following Hosenfeld et al. [40], we also calculated the bimodality coefficient (BC), which reflects the distribution of the graph densities. The BC ranges between zero and one, where a $BC > 0.55$ indicates a bimodal distribution, and a $BC < 0.55$ a unimodal distribution. The BC may also indicate whether or not a participant is at risk for a critical transition: an individual with an increased risk will have a distribution that resembles a bimodal distribution, whereas an individual with no increased risk will have a distribution that resembles a unimodal distribution [40].

Lastly, we use ML estimation to optimize p (Equation 7) from the data. A participant will have an increased risk for experiencing a critical transition when \hat{p} is smaller than the critical point. When \hat{p} is greater than the critical point, we conclude that the participant in question does not have an increased risk for experiencing a critical transition.

All analyses were performed using the R statistical software 3.3.1 [41]. Network visualization were done with the R-package qgraph version 1.3.5 [42]. Kernel densities for the BC are calculated in R using Silverman's rule of thumb [43] as default for the bandwidth parameter.

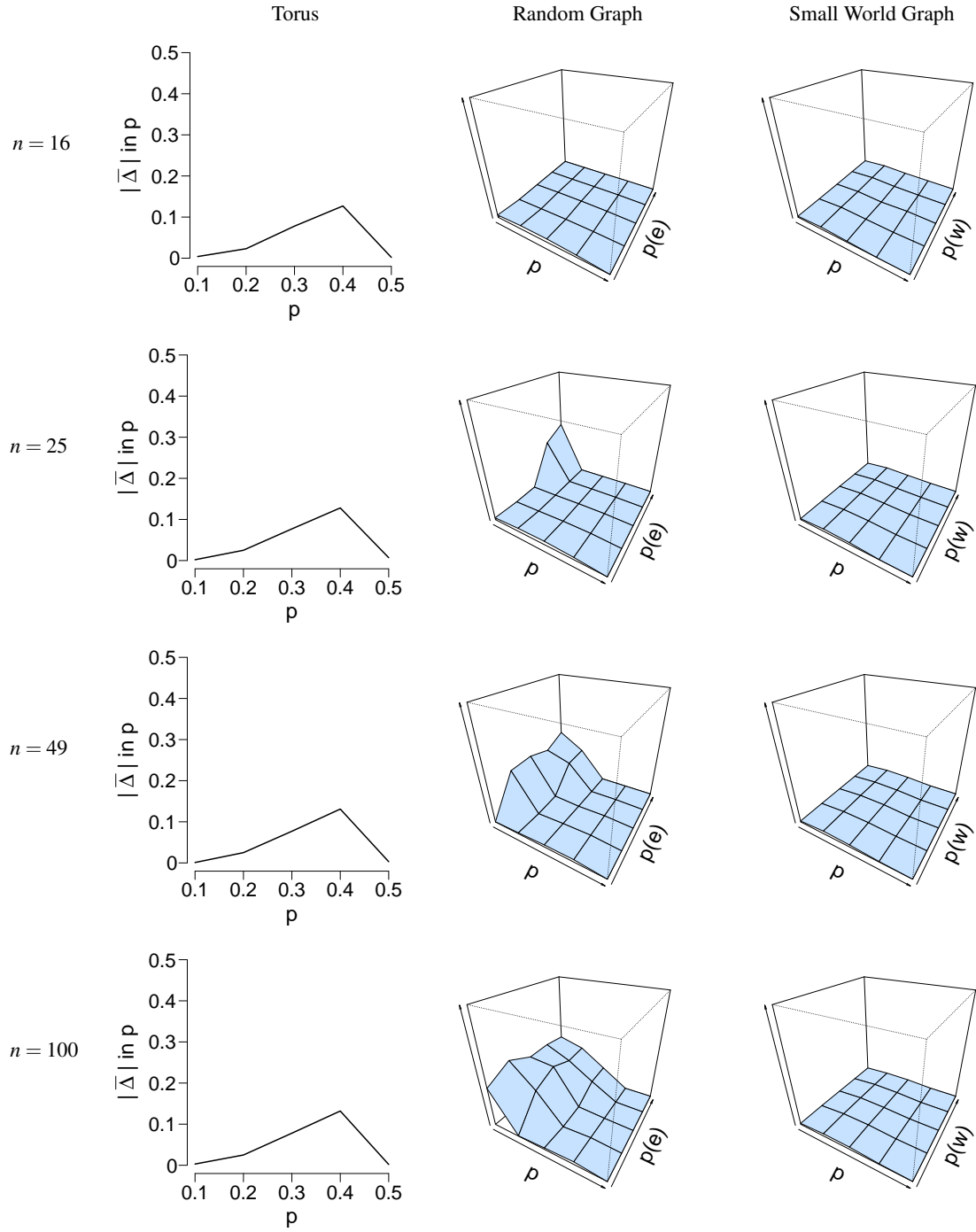


Figure 3: Visualization of the mean absolute differences between p and \hat{p} . Mean absolute difference is shown for a torus (left column), a random graph (middle column), and a small world graph (right column). For the left column, the x-axis denotes the parameter p for which we simulated data, and the y-axis the mean absolute difference between p and \hat{p} . For the middle and right column, the x-axis denotes the parameter p for which we simulated data, the y-axis the graph parameter that was used to simulate data, and the z-axis the mean absolute difference between p and \hat{p} .

A. Example 1: Extensive time-series data

Our first empirical example is a single-case study of a 57-year old man who has been suffering from major depressive disorder for more than eight years [13]. By means of ESM [6],

the participant's daily life experiences were monitored for 239 days. Ten times a day, the participant was asked to complete a 50-item questionnaire. See Kossakowski et al. [33] for a more detailed description of the data. It was shown in Wichers et al. [13] that the participant experienced a phase transition around

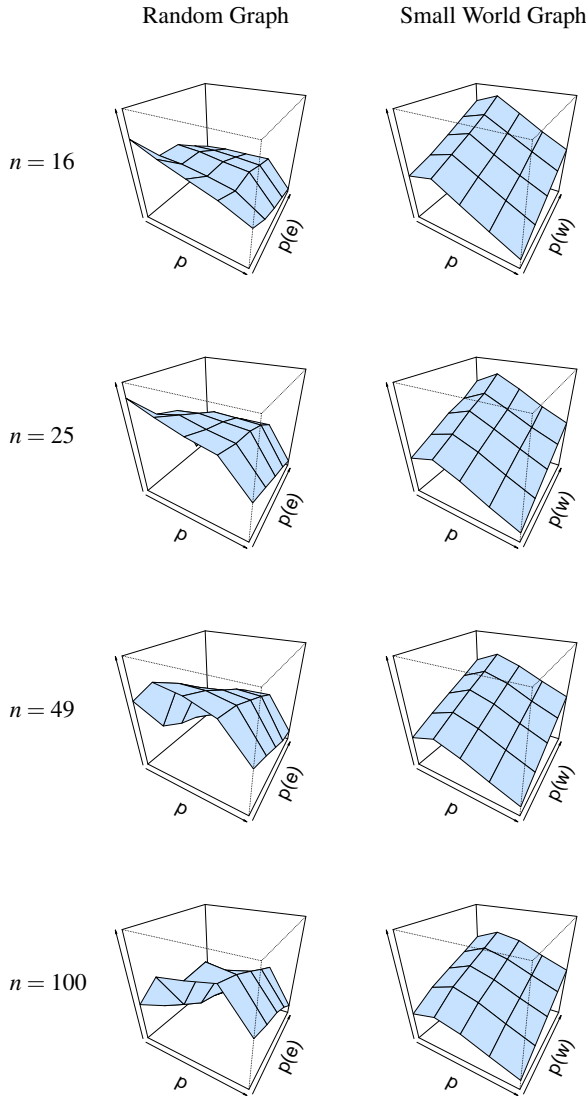


Figure 4: Visualization of the mean absolute differences between p_e and \hat{p}_e and p_w and \hat{p}_w . Mean absolute difference is shown for a random graph (left column) and a small world graph (right column). The x-axis denotes the parameter p for which we simulated data, the y-axis the graph parameter that was used to simulate data, and the z-axis the mean absolute difference between p and \hat{p} .

day 127. It is therefore an ideal dataset to validate whether the risk for experiencing a phase transition can be assessed. In order to validate our proposed method, it is necessary to only use the measurements prior to the phase transition, as we want to determine whether this participant showed an increased risk for experiencing a phase transition prior to the transition itself. Therefore, we only selected data up until the anti-depressant medication was reduced to 0 mg, which includes 671 time points.

We excluded 22 items from the entire analysis as they pertained to the social company the participant was in at the time

of the beep (9 items), an activity the participant engaged just before the beep (6 items), or a significant event that had taken place just before the beep (7 items). We included 28 items that measured the participants' mood, affect, self-esteem and physical condition, which were completed on 671 time points over a period of 14 weeks. Seven positive items were re-coded so that high scores indicate a more negative affect on all items. The included items were measured on a 7-point Likert scale, ranging from 1 (not) to 7 (very). Four items ('I feel down/lonely/anxious/guilty') were measured on a 7-point Likert scale, ranging from -3 (not) to +3 (very), as a pilot trial showed that this type of Likert scale resulted in more variation than the original Likert scale. For all 28 items, we dichotomised the data by means of a median split: scores below the median were marked '0', and scores above the median were marked '1'. After dichotomising the data, we determined the number of observations for each response category (0/1) and each item. In the case that one of the two response categories was observed less than four times, the item was removed. Three items were removed due to observing one of two response categories less than four times, ending up with a dataset that contains 25 items.

The network structure of this data is depicted in Figure 5 (upper panel). Item meanings and their assigned labels can be found in Table I. Positive associations are denoted by green edges, whereas negative associations are denoted by red edges. The thicker and more saturated the edge, the stronger the association [42]. It can be seen that all items are connected: the entire network has a connectivity of 0.27, meaning that 27% of all possible edges are nonzero. Also, item 12 (I feel strong) has strong connections to items 2 (I feel down), 17 (I like myself), 19 (I doubt myself) and 25 (I am sleepy), which means that, as item 12 increases, scores in items 2, 17, 19 and 25 tend to decrease, and vice versa. Also note that there is a strong positive association between items 2 (I feel down) and 15 (I worry); as the participant feels more down, he will also worry more and vice versa.

Figure 5 (middle panel) shows the evolution of the proportion of active nodes (density) throughout the entire data collection period. The black line depicts the period in which the anti-depressant medication was reduced, and the part of the data that we used to estimate p . The blue line marks the period in which no anti-depressant medication was taken by the participant. It can be seen that μ_p tends to behave in a wave-like pattern. Also, it can be seen that, when the participant does not take any anti-depressant medication, the wave-like pattern is getting more extreme: more peaks are observed, and the participants tends to 'stick' in those peaks more often.

The lower panel of Figure 5 depicts the bifurcation diagram accompanied by the estimation of p . It shows that \hat{p} is smaller than the critical point in this bifurcation diagram, indicating an increased risk for experiencing a critical transition. As we know that this participant actually experienced a critical transition around $T \approx 816$, this empirical example validates the proposed method for assessing the risk at a critical transition.

Figure 6 displays the distribution of the graph densities calculated for each time point using the included data. The bimodality coefficient (BC) for this participant is approximately

Item	Item meaning
1	I feel relaxed
2	I feel down
3	I feel irritated
4	I feel satisfied
5	I feel lonely
6	I feel anxious
7	I feel enthusiastic
8	I feel suspicious
9	I feel cheerful
10	I feel guilty
11	I doubt myself
12	I feel strong
13	I feel restless
14	I feel agitated
15	I worry
16	I can concentrate well
17	I like myself
18	I am ashamed of myself
19	I doubt myself
20	I can handle anything
21	I am hungry
22	I am tired
23	I am in pain
24	I have a headache
25	I am sleepy

Table I: Items that were included in the analysis and their assigned labels.

0.64, and thus resembles a bimodal distribution, a conclusion that is in line with our findings with respect to \hat{p} .

B. Example 2: Clinical sample

Data for our second empirical example were collected for a study in severely affected patients, admitted to a closed, psychiatric ward of an academic hospital [34, 35]. Participants were included in a previous study [34, 35] and have been described in detail in the associated papers. Participants ($N = 81$) completed the Dutch version of the Adjective Mood Scale [44] twice a day at fixed time points for a period of six weeks, resulting in a maximum of 84 measurements per participant. Participants had to indicate on this 28-item questionnaire which of either two mood states (or neither) corresponds most closely to the way participants were feeling at that moment in time. In the original design, the mood states were marked as ‘0’ or ‘2’, with ‘0’ indicating that this mood state is less applicable to the current situation, and ‘2’ meaning that this mood state corresponds more closely to the current situation. In the case that neither mood state corresponded to the current mood state, a ‘1’ was marked. Since these items all have two mood states, we decided to split all items up in a negative and positive component. When a participant indicated that his or her mood corresponded more closely to the positive component of the item, the positive component was marked with ‘1’ and the negative component with ‘0’. The reverse was performed when the participant indicated that his or

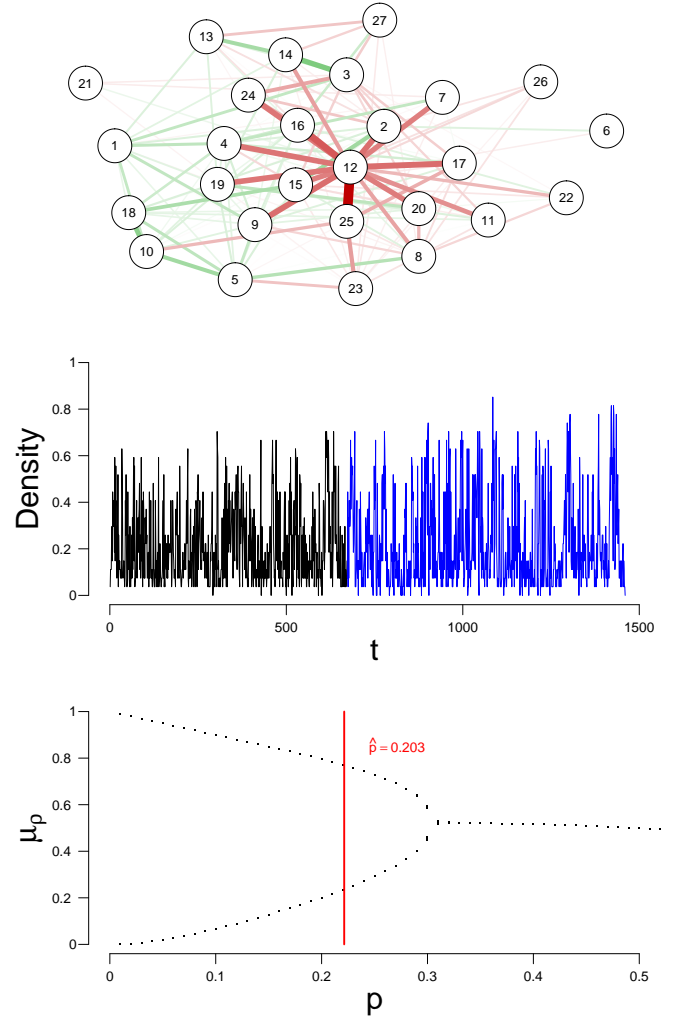


Figure 5: Network of the ESM data (upper panel), the evolution of the percentage of active nodes for each time point (middle panel), and the bifurcation diagram (lower panel). Item labels and their meanings can be found in Table I. The size of the associations between two nodes in the network in the upper panel is represented using the color and thickness of an edge, where positive associations are represented by green, and negative associations by red. The black line in the middle panel depicts the period in which anti-depressant medication was reduced, the blue line depicts the period in which no anti-depressant medication was taken. The red line in the bifurcation diagram in the lower panel indicates the estimation of p . μ_p = the expected density calculated with equation (4).

her mood corresponded more closely to the negative component of the item. When the participant indicated that neither of the mood states fit his or her current mood state, a ‘0’ was marked. Figure 7 shows a visualization and an example of the split strategy that was used. Using this split strategy, we ended up with 56 binary items.

For clarity of presentation, we present the results of solely

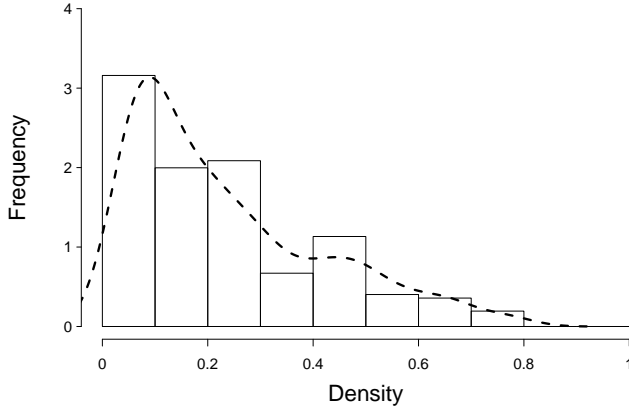


Figure 6: Distribution of the graph densities calculated at each time point. The dashed line represents the Kernel density of the distribution.

Item	Item meaning
1	I currently feel refreshed/listless*
2	I currently feel indifferent toward others/interested in others
3	I currently feel pleased/depressed*
4	I currently feel successful/unsuccessful*
5	I currently feel irritable/peaceful
6	I currently feel indecisive/ready to make decisions
7	I currently feel cheerful/tearful*
8	I currently feel in a good mood/in a bad mood*
9	I currently feel lacking in appetite/with a good appetite
10	I currently feel sociable/withdrawn*
11	I currently feel unworthy/worthy
12	I currently feel relaxed/tense*
13	I currently feel happy/unhappy*
14	I currently feel shy/communicative
15	I currently feel sinful and wicked/pure
16	I currently feel secure/threatened*
17	I currently feel abandoned/cared for
18	I currently feel even-tempered/driven**
19	I currently feel confident/insecure*
20	I currently feel miserable/comfortable
21	I currently feel flexible/inflexible*
22	I currently feel tired/rested
23	I currently feel hesitant/firm
24	I currently feel calm/restless*
25	I currently feel lacking in energy/energetic
26	I currently feel useless/indispensable
27	I currently feel sluggish/lively
28	I currently feel superior/inferior*

Table II: Items of the Adjective Mood Scale (AMS) and their assigned labels.* Items that have a reversed response scale.

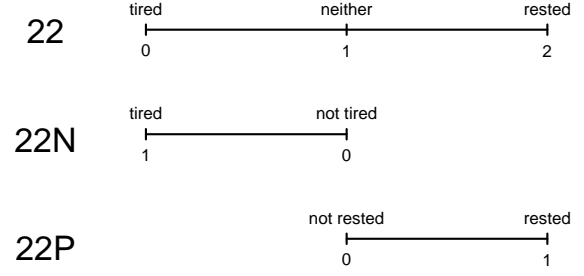


Figure 7: Schematic representation of the split strategy used to recode score on the Adjective Mood Scale (AMS) questionnaire. 22 = original item. 22N = new item, negative component. 22P = new item, positive component.

those participants who had a percentage of missing data lower than 10%, and whose network structure did not include any isolated nodes. Isolated nodes cannot transport any information throughout the network, and thus cannot be used to assess the risk for experiencing a phase transition. Three participants satisfied both inclusion criteria, and are thus included in our analysis. Note that these inclusion criteria are strict to have rather ideal cases to demonstrate how the mean field approximation would pan out in such cases. Table III depicts the demographic information about the selected participants. Results from all participants that were not selected for this paper can be found online [27].

As described earlier, we replaced missing item scores with the scores at the previous time point. Since the items are already dichotomous, the step of dichotomising the items was skipped. For each item, we determined the number of observations for each response category (0/1) and each item. In the case that one of the two response categories was observed less than four times, the item was removed. For the first participant, no items were removed, ending up with a dataset that contains 56 items. For the second participant, 5 items were removed due to observing one of two response categories less than four times, ending up with a dataset that contains 51 items. Finally, for the third participant, 13 items were removed due to observing one of two response categories less than four times, ending up with a dataset that contains 43 items.

Figure 8 depicts the network structure of the three participants. Each network has been given the same layout to improve the visual comparison of the networks. Item labels can be found in Table II. Positive associations are denoted by green edges, whereas negative associations are denoted by red edges. The thicker and more saturated the edge, the stronger the association [42]. Note that node labels ending with 'P' denote the positive component of the items, and node labels ending with 'N' the negative component of the items. It can be seen that positive and negative components of the same item tend to be highly negatively correlated, which makes sense: an increase in the positive component automatically means a decrease in the negative component of items.

	Participant 1	Participant 2	Participant 3
Gender	Female	Female	Female
DSM-III-R diagnosis	Severe major depressive disorder with psychotic features	Severe major depressive disorder, single episode with psychotic features	Bipolar disorder, not otherwise specified
Age at admission	43	30	55
Admission period	144 days	120 days	61
No. time points	84	84	84
% missing data	5.95%	7.14%	0.00%

Table III: Descriptive information of the participants.

Moreover, for the first participant (upper row), a strong association exists between items 5P (I currently feel peaceful) and 19P (I currently feel confident). For the second participant (middle row), a strong association exists between items 9N (I currently feel lacking in appetite) and 27N (I currently feel sluggish). For the third participant (lower row), a strong association exists between items 8N (I currently feel in a bad mood) and 23N (I currently feel hesitant).

Interestingly, the network's connectivity indices were quite similar: the network in the upper row has a connectivity of 0.047, the middle network a connectivity of 0.06 and the lower network a connectivity of 0.066. This means that either 4.7%, 6.0% or 6.6% of all possible edges are nonzero. When we look at the global strength, the sum of the absolute edge weights, we see that the network of participant one has a global strength of 241, the network of participant two a global strength of 243, and the network of participant three a global strength of 166. This finding may point towards a pattern demonstrated by van Borkulo et al. [45], where it was found that participants whose depression was in remission displayed a less strong connected network in comparison to participants whose depression persisted.

Figure 9 (left column) shows the evolution of the proportion of active nodes (density) throughout time for three different participants. It can be seen that the participants' trajectory differ quite somewhat. All participants show some sort of systematic pattern with respect to the density. The first participant (upper row) displays the most variation, and the second participant (middle row) hardly any variation. The right column of Figure 9 depicts the bifurcation diagrams, accompanied by the person-specific estimation of p . Note that an increased risk for experiencing a critical transition in these data may suggest that these participants have an increased risk to experience a critical transition from a depressed mood state to a healthy mood state. If such an increased risk is not found, it may indicate that these participants, based on the data, do not have an increased risk for experiencing a critical transition from a depressed mood state to a healthy mood state. For all participants, \hat{p} is higher than the critical point, which means that these participants do not have an increased risk for experiencing a critical transition from a depressed to a healthy mood state.

Figure 10 displays the distribution of the graph densities calculated for each time point using the included data. For each participants we calculated the bimodality coefficient (BC); a BC higher than 0.55 indicates an increased risk for

Scale	Mean (SD)	Range
DASS depression	6.66 (4.92)	0 - 42
DASS anxiety	7.88 (8.44)	0 - 36
DASS distress	4.37 (5.38)	0 - 40
QIDS	9.73 (7.39)	0 - 25

Table IV: Means, standard deviations (SD) and the range on various (sub) scales. DASS = Depression Anxiety Stress Scale, QIDS = Quick Inventory of Depressive Symptomatology.

a critical transition, and a BC lower than 0.55 indicates the absence of this risk. The BC for the first participant (upper panel) is 0.99, for the second participant (middle panel) 0.53 and for the third participant (lower panel) 0.67. Contrary to our findings based on the p estimate \hat{p} , the BCs of the first and third participant indicate a bimodal distribution, and therefore an increased risk for a critical transition, whereas the BC of the second participant indicates a unimodal distribution. and with that no increased risk for a critical transition.

C. Example 3: General sample

Participants were originally recruited in a nation-wide study called HoeGekIsNL (in English: HowNutsAreTheDutch) [46] and have been described in detail in a previous paper [36]. Participants ($N = 975$) completed Dutch versions of the Depression Anxiety Stress Scale (DASS) [47, 48] and the Quick Inventory of Depressive Symptomatology (QIDS) [49, 50] before proceeding to the data collection. For a period of 31 days, participants filled out 43 items three times a day at fixed time points, resulting in a maximum of 93 measurements for each participant [36]. Sum scores were calculated for (sub) scales of the questionnaires; a summary is shown in Table IV.

For clarity of presentation, we present the results of three participants. Based on the cut-off scores of the QIDS and the DASS, as found in the associated scoring manuals, participants were categorized into one of five groups for each (sub) scale. The categorization scheme can be found in Table V. We included participants who were categorized as normal on all (sub) scales, participants who were categorized as mild on the DASS anxiety sub scale, and moderate on all others, and participants who were categorized as extremely severe on all (sub) scales). We chose a mix of mild and moderate scores

for the middle group as no participants were categorized as mild for both the QIDS and the DASS. The one participant who was categorized as moderate for the QIDS and the DASS turned out only to have three measurements, which is too little to analyse. This participant was thus excluded from the entire analysis.

This selection procedure resulted in 299 participants: 297 in the normal group, two in the mild group, and one in the severe group. Within these groups, we selected those participants who had a percentage of missing data lower than 10%, and whose network structure did not include any isolated nodes. Isolated nodes cannot transport any information throughout the network, and thus cannot be used to assess the risk for experiencing a critical transition. Three participants satisfied both inclusion criteria, and are thus included in our analysis. Note that these inclusion criteria are strict to have rather ideal cases to demonstrate how the mean field approximation would pan out in such cases. Also, in the mild group, one participant turned to have no diary measurements whatsoever, leaving us with only one eligible participant that we selected, regardless of the percentage of missing data. As the severe group only contained one participant, this participant was automatically selected, regardless of the percentage of missing data. Table VI shows the demographic information about the selected participants. Results from all participants that were not selected for this paper can be found online [27].

As described earlier, we replaced missing item scores with the scores at the previous time point. Items were dichotomised using a median split. For each item, we determined the number of observations for each response category (0/1) and each item. In the case that one of the two response categories was observed less than four times, the item was removed. For the first participant, one item removed due to observing one of two response categories less than four times, ending up with a dataset that contains 22 items. For the second and third participant, no items were removed due to observing one of two response categories less than four times, which leaves us with a dataset that contains 23 items.

Figure 11 depicts the network structure of the three participants. The upper row depicts the participant from the normal group, the middle row the participant from the mild group, and the lower row the participant from the severe group. Item labels and their meaning can be found in Table VII. Each network has been given the same layout to improve the visual comparison of the networks. For the participant in the upper row, strong negative associations exist between items 6 (I feel nervous) and 1 (I feel relaxed), 7 (I feel content), 13 (I feel valued), and 20 (I feel unbalanced). Also, a strong positive association exists between item 6 and 16 (I feel confident). This means that, as item 6 changes, these items change accordingly. For the participant in the middle row, item 10 (I feel dull) has a strong positive associations with item 12 (I feel tired), and strong negative associations with items 1 (I feel relaxed) and 13 (I feel valued). For the participant in the lower row, strong positive associations exist between items 1 (I feel relaxed) and 9 (I feel calm). Also, item 16 (I feel confident) has strong negative associations with items 17 (I worry a lot), 19 (I feel my life is worth living) and 20 (I am unbalanced).

Interestingly, the network's connectivity are quite similar: the network in the upper row has a connectivity of 0.195, the middle network a connectivity of 0.198 and the lower network a connectivity of 0.19. This means that either 19.5%, 19.8% or 19.0% of all possible edges are nonzero. It can also be seen that the global strength of the network increases from left to right: the participant in the upper row has a global strength of 204, the participant in the middle row a global strength of 326 and the participant in the lower row a global strength of 492. This finding may point towards a pattern demonstrated by van Borkulo et al. [45], where they found that participants with persistent depression displayed a more strongly connected network in comparison to participants who were in remission.

Figure 12 (left column) shows the evolution of the proportion of active nodes (μ_p) throughout time for three different participants. It can be seen that the participants' trajectory are somewhat similar. The participants in the middle and lower row show a similar pattern, with lots of variability. The participant in the upper row also varies quite somewhat, but at the same time, it can be seen that this participant shows a decreasing pattern. The right column of Figure 12 depicts the bifurcation diagrams, accompanied by the person-specific estimation of p . For all participants, \hat{p} is higher than the critical point, which means that these participants do not have an increased risk for experiencing a critical transition from a healthy to a depressed mood state.

Figure 13 displays the distribution of the graph densities calculated for each time point using the included data. For each participants we calculated the BC; a BC higher than 0.55 indicates an increased risk for a critical transition, and a BC lower than 0.55 indicates the absence of this risk. The BC for the first participant (upper panel) is 0.41, for the second participant (middle panel) 0.38 and for the third participant (lower panel) 0.31. In line with our findings based on the p estimate \hat{p} , all participants' distributions resemble a unimodal distribution, and thus show no increased risk for a critical transition based on the BC.

VI. DISCUSSION

In this paper, we demonstrated the potential of the mean field approximation, by applying it to three different empirical examples. In a validation study, it was shown that p and p_w are accurately estimated by the model. By giving three different empirical examples, we demonstrated how the mean field approximation works in practice, by applying it to not only a sample from the clinical population and a sample from the general population, but also to a participant from which it was known that the participant experienced a phase transition. Results from that analysis validates the approach that we took in assessing the risk for a phase transition.

For each participant, we estimated Ising models, by assuming that all measurements are independent of each other. However, this assumption may be hard to satisfy when questionnaires are completed several times a day. It is possible that participants will think back to the last completed ques-

Scale	Symptom severity				
	Normal	Mild	Moderate	Severe	Extremely severe
DASS depression	0-9	10-13	14-20	21-27	> 27
DASS anxiety	0-7	8-9	10-14	15-19	> 19
DASS stress	0-14	15-18	19-25	26-33	> 33
QIDS	0-5	6-10	11-15	16-20	> 27

Table V: Categorization scheme of the QIDS and the DASS. Scores depict sum scores. DASS = Depression Anxiety Stress Scale, QIDS = Quick Inventory of Depressive Symptomatology.

	Participant 1	Participant 2	Participant 3
Gender	Female	Female	Female
Date of birth	March 1954	February 1990	March 1979
Age at start diary collection	62.19	24.49	45.48
No. time points	78	93	90
% missing data	0.00%	13.97%	16.67%

Table VI: Descriptive information of the included participants.

Item	Item meaning
1	I feel relaxed
2	I feel gloomy
3	I feel energetic
4	I feel anxious
5	I feel enthusiastic
6	I feel nervous
7	I feel content
8	I feel irritable
9	I feel calm
10	I feel dull
11	I feel cheerful
12	I feel tired
13	I feel valued
14	I feel lonely
15	I feel I fall short
16	I feel confident
17	I worry a lot
18	I am easily distracted
19	I feel my life is worth living
20	I am unbalanced
21	I am in the here and now
22	My appetite is..
23	Since the last measurement I had a laugh

Table VII: Items that were included in the analysis and their assigned labels.

tionnaire, and complete the new questionnaire in light of the previous one. As measurements are possibly dependent, this could result in a bias in the network estimation. This bias can be more apparent when participants are asked to complete ten questionnaires a day in comparison to only two questionnaires a day. Future research should thus focus on developing a more robust estimation procedure that does not include the assumption of independent measurements.

In both the clinical and the general sample, results showed that all participants did not have an increased risk for experiencing a critical transition. For both these samples, there was

no follow-up to see whether or not these participants actually experienced a critical transition. In the case of the clinical sample, a follow-up may reveal whether patients, who show an increased risk for a critical transition, actually underwent that transition in order to return to a healthy mood state again. For the general sample, it is unclear whether participants already received a clinical diagnosis. It could very well be the case that participant who scored high on the depression questionnaires, but did not show an increased risk for a critical transition, may already be clinically depressed, or just are in a bad place during the data collection. Without any follow-up, it is hard to tell what caused the results, and what the results actually mean. For future research, it is important to include a follow-up measurement when collecting ESM-data for these purposes, so that we gain more insight into the causes and consequences of the found results.

When collecting time-series data, participants are requested multiple times a day to fill out a questionnaire for a certain period. This type of data collection demands time and energy of the participants. It thus makes sense that participants sometimes forget to complete a questionnaire, or are simply not up for it at that specific moment, for whatever reason. In the data that we analysed, we came across different ratios of missing data and completed measurements. In this paper it was assumed that the response scores did not change at the missing measurement, and as a result, missing measurements were replaced by the previous one. Adopting this approach for handling missing data also decreases the variance that individual items may have, thereby increasing the probability that items need to be removed due to too little variance. At this point in time, there is no clear picture of the effects of missing data in time-series analysis like the one proposed and applied in this paper. Future research should focus on mapping the effects that different types of missing data have on time-series analysis, and what the effect of various imputation methods have on the analyses.

In this paper, we assumed all network structures to be random graphs. Ideally, we would want to be able to distinguish between different types of network structures, by using a test.

We ran a validation study to test whether we can make this distinction by comparing the network's degree distribution with a simulated degree distribution of a similar network structure. Results of this study showed that using the degree distribution to distinguish between a small world graph and a random graph is not possible. Future research could focus on developing such a test, as Waldorp and Kossakowski [3] showed that the bifurcation diagrams are not all that similar, and different conclusions can be made when using a different network structure.

Prior to our analysis, the data underwent many preprocessing steps. Data had to be dichotomized, all response categories had to be observed at least four times within individual item, and missing data had to be imputed, since the current method does not allow for missing data. These steps are necessary, but possibly unrealistic at this point in time. The method proposed in this paper is currently only accessible for 'perfect' binary data. However, data are often imperfect: low variance as well as missing data occurs recurrently in time-series data. More importantly, it can be argued that MDD symptoms may not be binary, but categorical or even continuous. Our method, currently, does not account for the possible variation in MDD symptoms that may occur within individuals: an individual either experiences or does not experience insomnia (one of the MDD symptoms as listed in the Diagnostic and Statistical Manual of Mental Disorders [51]), regardless of the severity of the insomnia that is experienced. We hope to expand the mean field approximation as presented in this paper so that we may account for the variation within MDD symptoms by allowing for categorical or continuous items, as well as items with low variance or missing data.

In conclusion, our findings indicate that the mean field approximation is capable in properly assessing the risk that individuals may have in experiencing a critical transition.

The proposed method could potentially aid clinical therapists by giving information about the risk for a critical transition that patients suffering from MDD may have, and therefore the 'risk' that patients may have in transitioning back into a healthy phase. Also, individuals that have recovered from MDD can potentially be assisted by monitoring their risk for a relapse in MDD.

ACKNOWLEDGMENTS

This research was supported by European Research Council Consolidator Grant no. 647209.

JK is partly funded by the Research Priority Area Yield, part of the Research Institute of Child Development and Education, University of Amsterdam, the Netherlands.

The single-case experiment was designed by Marieke Wichers and Peter Groot. This study was supported by an Aspasia grant (MW., NWO grant), and by the Brain Foundation of the Netherlands (MW., grant No. F2012(1)-03).

The work on the HowNutsAreTheDutch project was supported by the Netherlands Organization for Scientific Research (NWO-ZonMW), by a VICI grant entitled Deconstructing Depression (no: 91812607) received by Prof. Dr. Peter de Jonge. Part of the HowNutsAreTheDutch project was realized in collaboration with the Espria Academy. We want to thank all participants of the HowNutsAreTheDutch project for their participation and valuable contribution to this research project.

We thank Marieke Wichers and the HowNutsAreTheDutch project for letting us use their data. We also want to express our gratitude to Peter Groot, all the participants of the HowNutsAreTheDutch project, and the patients of the closed ward. The authors thank Marieke Wichers, Pia Tio and Maarten Marsman for their contributions to the manuscript.

-
- [1] World Health Organization. Depression, a hidden burden. Retrieved from: <http://www.who.int>, 2012.
 - [2] Peter de Jonge, Henk J Conradi, Kirsten I Kaptein, Claudi LH Bockting, Jakob Korf, and Johan Ormel. Duration of subsequent episodes and periods of recovery in recurrent major depression. *Journal of Affective Disorders*, 125:141–145, 2010.
 - [3] Lourens J Waldorp and Jolanda J Kossakowski. Mean Field Dynamics of Graphs I: Evolution of Probabilistic Cellular Automata on Different Types of Graphs. Submitted for publication, 2017.
 - [4] Angélique O J Cramer, Sophie Sluis, Arjen Noordhof, Marieke Wichers, Nicole Geschwind, Steven H Aggen, Kenneth S Kendler, and Denny Borsboom. Dimensions of normal personality as networks in search of equilibrium: You can't like parties if you don't like people. *European Journal of Personality*, 26: 414–431, 2012.
 - [5] László Gulyás, George Kampis, and Richard O Legendi. Elementary models of dynamic networks. *The European Physical Journal Special Topics*, 222(6):1311–1333, 2013.
 - [6] Mihaly Csikszentmihalyi and Reed Larson. Validity and reliability of the experience-sampling method. *The Journal of Nervous and Mental Disease*, 175:137–193, 1987.
 - [7] Peter Kuppens and Philippe Verduyn. Looking at Emotion Regulation Through the Window of Emotion Dynamics. *Psychological Inquiry*, 26:72–79, 2015.
 - [8] C Telford, S McCarthy-Jones, R Corcoran, and G Rowse. Experience Sampling Methodology studies of depression: the state of the art. *Psychological Medicine*, 42:1119–1129, 2011.
 - [9] Marije aan het Rot, Koen Hogenelst, and Robert A Schoevers. Mood disorders in everyday life: A systematic review of experience sampling and ecological momentary assessment studies. *Clinical Psychology Review*, 32:510–523, 2012.
 - [10] Marten Scheffer, Jordi Bascompte, William A Brock, Victor Brovkin, Stephen R Carpenter, Vasilis Dakos, Hermann Held, Egbert H van Nes, Max Rietkerk, and George Sugihara. Early-warning signals for critical transitions. *Nature*, 46:53–59, 2014.
 - [11] Yuri A Kuznetsov. *Elements of applied bifurcation theory*. New York, USA: Springer-Verlag, 2013.
 - [12] Ingrid A van de Leemput, Marieke Wichers, Angélique O J Cramer, Denny Borsboom, Francis Tuerlinckx, Peter Kuppens, Egbert H van Nes, Wolfgang Viechtbauer, Erik J Giltay, Steven H Aggen, Catherine Derom, Nele Jacobs, Kenneth S

- Kendler, Han L J van der Maas, Michael C Neale, Frenk Peeters, Evert Thiery, Peter Zachar, and Marten Scheffer. Critical Slowing Down as Early Warning for the Onset and Termination of Depression. *Proceedings of the National Academy of Sciences*, 111:87–92, 2014.
- [13] Marieke Wichers, Peter C Groot, Psychosystems, ESM Group, and ESW Group. Critical Slowing Down as a Personalized Early Warning Signal for Depression. *Psychotherapy and Psychosomatics*, 85:114–116, 2016.
- [14] Stephen Wolfram. Computation theory of cellular automata. *Communications in Mathematical Physics*, 96(1):15–57, 1984.
- [15] Palash Sarkar. A brief history of cellular automata. *ACM Computing Surveys (CSUR)*, 32(1):80–107, 2000.
- [16] Geoffrey Grimmett. *Probability on graphs: random processes on graphs and lattices*, volume 1. Cambridge University Press, 2010.
- [17] Joel L Lebowitz, Christian Maes, and Eugene R Speer. Statistical mechanics of probabilistic cellular automata. *Journal of Statistical Physics*, 59:117–170, 1990.
- [18] Robert Kozma, Marko Puljic, Paul Balister, Béla Bollobás, and Walter J Freeman. Phase transitions in the neuropercolation model of neural populations with mixed local and non-local interactions. *Biological Cybernetics*, 92:367–379, 2005.
- [19] Paul Balister, Béla Bollobás, and Robert Kozma. Large deviations for mean field models of probabilistic cellular automata. *Random Structures & Algorithms*, 29:399–415, 2006.
- [20] Morris W Hirsch, Stephen Smale, and Robert L Devaney. *Differential equations, dynamical systems, and an introduction to chaos*. Academic press, 2012.
- [21] Béla Bollobás. *Random Graphs*. Cambridge, UK: Cambridge University Press, 2001.
- [22] Rick Durrett. *Random Graph Dynamics*. Cambridge, UK: Cambridge University Press, 2007.
- [23] Duncan J Watts and Steven H Strogatz. Collective dynamics of small-world’ networks. *Nature*, 393:440–442, 1998.
- [24] M E C Newman and D J Watts. Renormalization group analysis of the small-world network model. *Physics Letters A*, 263:4–6, 1999.
- [25] M B Rajarshi. *Statistical Inference for Discrete Time Stochastic Processes*. Springer, 2012.
- [26] Thomas R Fleming and David P Harrington. Estimation for discrete time nonhomogeneous Markov chains. *Stochastic Processes and their Applications*, 7:131–139, 1978.
- [27] Jolanda J Kossakowski. Results from ‘Mean Field Dynamics of Graphs II: Assessing the Risk for the Development of Phase Transitions in Empirical Data’. Retrieved from <https://osf.io/edyzpl/>, 2016.
- [28] S Milgram. The small world problem. *Psychology Today*, 2: 60–67, 1967.
- [29] M E J Newman, Duncan J Watts, and Steve H Strogatz. Random graph models of social networks. *Proceedings of the National Academy of Sciences of the United States of America*, 99:2566–2572, 2002.
- [30] MO Jackson. *Social and Economic Networks*. Princeton University Press, Princeton, USA, 2008.
- [31] Denny Borsboom, Angélique O J Cramer, Verena D Schmittmann, Sacha Epskamp, and Lourens J Waldorp. The small world of psychopathology. *PloS ONE*, 6(11):e27407, 2011.
- [32] Pia Tio, Sacha Epskamp, Arjen Noordhof, and Denny Borsboom. Mapping the manuals of madness: Comparing the ICD10 and DSMIVTR using a network approach. *International Journal of Methods in Psychiatric Research*, 2016. doi: 10.1002/mpr.1503.
- [33] Jolanda J Kossakowski, Peter C Groot, Jonas M B Haslbeck, Denny Borsboom, and Marieke Wichers. Data from Critical Slowing Down as a Personalized Early Warning Signal for Depression’. *Journal of Open Psychology Data*, 5:1–3, 2017. doi: <https://doi.org/10.5334/jopd.29>.
- [34] MCM Gordijn, DGM Beersma, AL Bouhuys, E Reinink, and RH van den Hoofdakker. A longitudinal study of diurnal mood variation in depression: characteristics and significance. *Journal of Affective Disorders*, 31:261–273, 1994.
- [35] MCM Gordijn, DGM Beersma, AL Bouhuys, and RH van den Hoofdakker. Mood variability and sleep deprivation effect as predictors of therapeutic response in depression. *Sleep-wake research in the Netherlands*, 9:41–44, 1998.
- [36] L van der Krieke, Bertus F Jeronimus, Frank J Blaauw, Rob B K Wanders, Ando C Emerencia, Hendrika M Schenk, Stijn de Vos, Evelien Snippe, Marieke Wichers, Johanna T W Wigman, Elisabeth H Bos, Klaas J Wardenaar, and Peter de Jonge. HowNutsAreTheDutch (HoeGekIsNL): A crowdsourcing study of mental symptoms and strengths. *International Journal of Methods in Psychiatric Research*, 25:123–144, 2015.
- [37] Claudia van Borkulo, Sacha Epskamp, and with contributions from Alexander Robitzsch. IsingFit: Fitting Ising models using the eLasso method, 2014. URL <http://cran.r-project.org/package=IsingFit>.
- [38] Claudia D van Borkulo, Denny Borsboom, Sacha Epskamp, Tessa F Blanken, Lynn Boschloo, Robert A Schoevers, and Lourens J Waldorp. A New Method for Constructing Networks from Binary Data. *Scientific reports*, 4:1–10, 2014.
- [39] Pradeep Ravikumar, Martin J Wainwright, and John D. Lafferty. High-dimensional Ising model selection using 1-regularized logistic regression. *the Annals of Applied Statistics*, 38:1287–1319, 2010.
- [40] Bettina Hosenfeld, Elisabeth H Bos, Klaas J Wardenaar, Henk J Conradi, Han L J van der Maas, Ingmar Visser, and Peter de Jonge. Major depressive disorder as a nonlinear dynamic system: bimodality in the frequency distribution of depressive symptoms over time. *BMC Psychiatry*, 15:1–9, 2015.
- [41] R Core Team. R: A Language and Environment for Statistical Computing, 2016. URL <https://www.r-project.org/>.
- [42] Sacha Epskamp, Angélique O J Cramer, Lourens J Waldorp, Verena D Schmittmann, and Denny Borsboom. qgraph: Network Visualizations of Relationships in Psychometric Data. *Journal of Statistical Software*, 48:1–18, 2012. URL <http://www.jstatsoft.org/v48/i04/>.
- [43] B W Silverman. *Density estimation*. Chapman and Hall, London, UK, 1986.
- [44] DV von Zerssen. Clinical self-rating scales (CSRS) of the Munich psychiatric information system (PSYCHIS M{ü}nchen). In *Assessment of depression*, pages 270–303. Springer, 1986.
- [45] Claudia D van Borkulo, Lynn Boschloo, Denny Borsboom, Brenda W J H Penninx, Lourens J Waldorp, and Robert A Schoevers. Association of symptom network structure with the course of depression. *JAMA Psychiatry*, 72:1219–1226, 2015.
- [46] Interdisciplinary Center for Psychopathology and Emotion Regulation. Hoe gek is Nederland? Retrieved from <https://www.hoegekis.nl/>.
- [47] PF Lovibond and SH Lovibond. The structure of negative emotional states - comparison of the depression anxiety stress scale (DASS) with the beck depression and anxiety inventories. *Behaviour Research and Therapy*, 33:335–343, 1995.
- [48] SH Lovibond and PF Lovibond. *Manual for the depression anxiety stress scales*. Psychology Foundation, Sydney, Australia, 2nd editio edition, 1995.
- [49] A Rush, M Trivedi, H Ibrahim, T Camody, B Arnow, D Klein,

- J Markowitz, P Ninan, S Kornstein, R Manber, M Thase, J Kocsis, and M Keller. The 16-item quick inventory of depressive symptomatology (QIDS), clinician rating (QIDS-C), and self-report (QIDS-SR): a psychometric evaluation in patients with chronic major depression. *Biological Psychiatry*, 54:573–583, 2003.
- [50] A Rush, L Bernstein, M Trivedi, T Camody, S Wisniewski, J Mundt, K Shores-Wilson, M Biggs, A Woo, A Nierenberg, and M Fava. An evaluation of the quick inventory of depressive symptomatology and the Hamilton rating scale for depression: a sequenced treatment alternatives to relieve depression trial report. *Biological Psychiatry*, 59:493–501, 2006.
- [51] American Psychiatric Association. *Diagnostic and statistical manual of mental disorders (DSM-5®)*. American Psychiatric Pub, 2013.

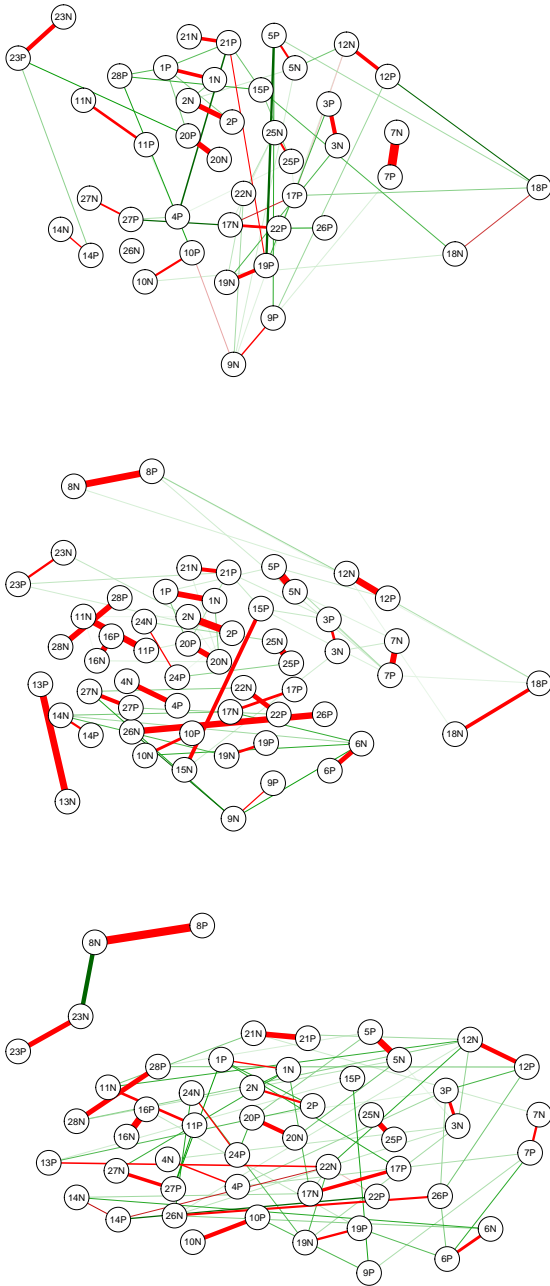


Figure 8: Networks of three participants of the clinical sample. Each row depicts a participant. The size of the associations between two nodes in the networks is represented using the color and thickness of an edge, where positive associations are represented by green, and negative associations by red. Item labels can be found in Table II.

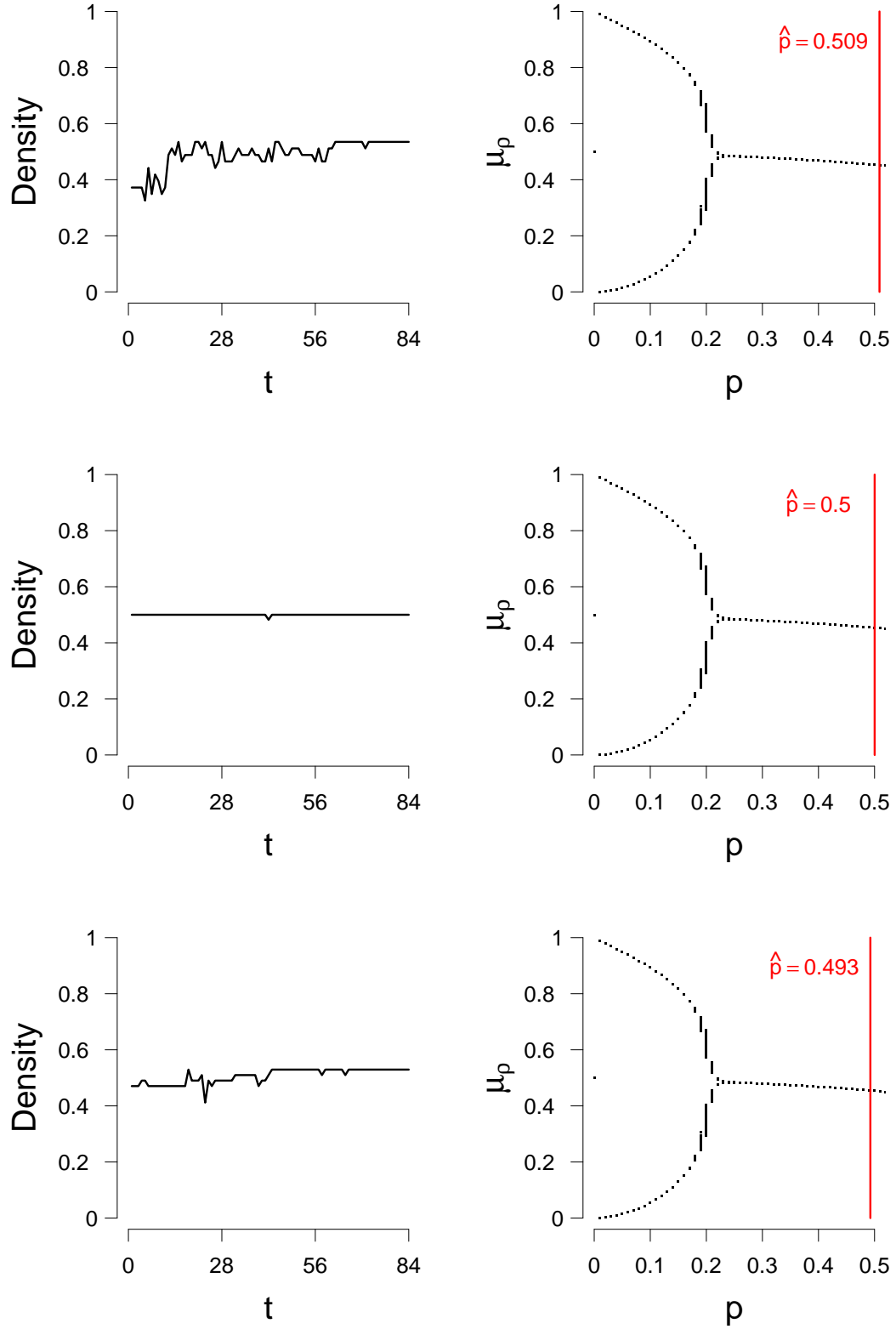


Figure 9: The evolution of the percentage of active nodes for each time point (left column), and the bifurcation diagram (right column). Each row depicts a participant. The red line in the bifurcation diagram indicates the estimate of p . μ_p = the expected density calculated with equation (4).

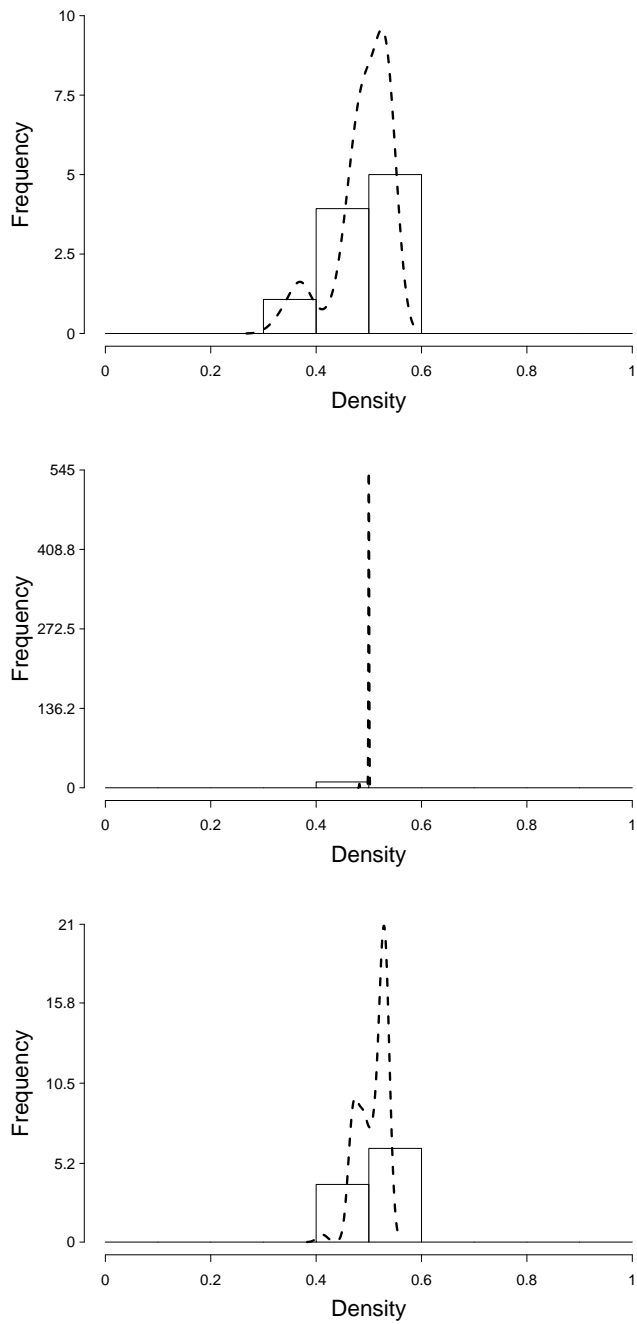


Figure 10: Distributions of the graph densities calculated at each time point for the three participants of the clinical sample. The dashed line represents the Kernel density of the distribution.

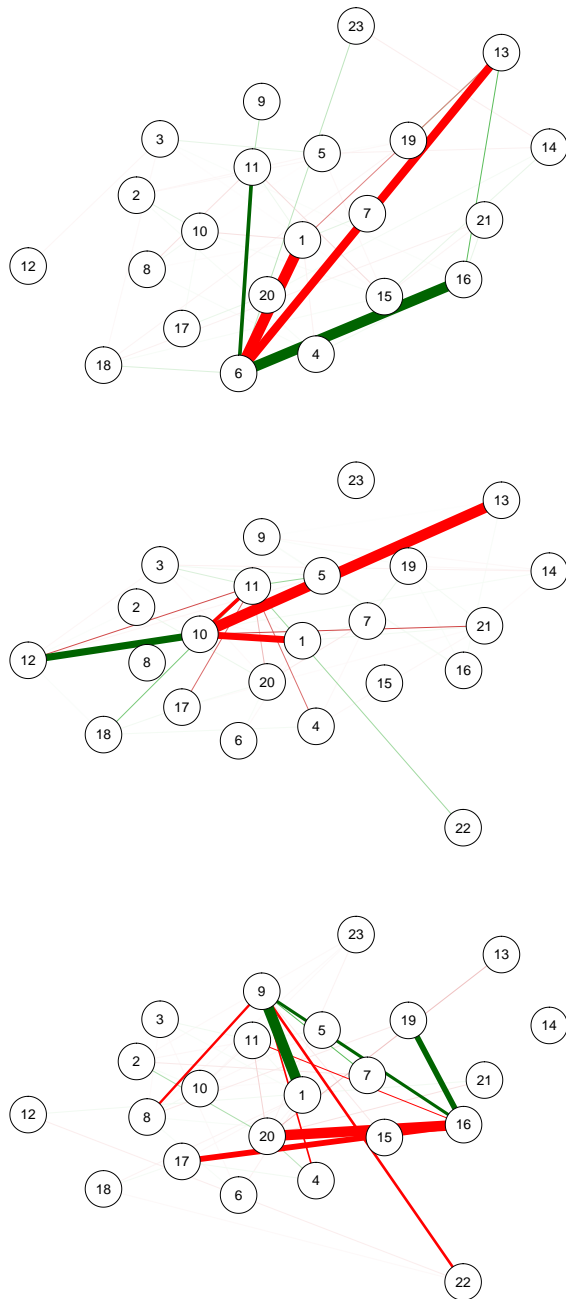


Figure 11: Networks of three participants of the general sample. Each row depicts a participant. The size of the associations between two nodes in the networks is represented using the color and thickness of an edge, where positive associations are represented by green, and negative associations by red. Upper row = participant from the low-group. Middle row = participant from the medium-group. Lower row = participant from the high-group. Item labels correspond to the original item numbers are given in Table VII.

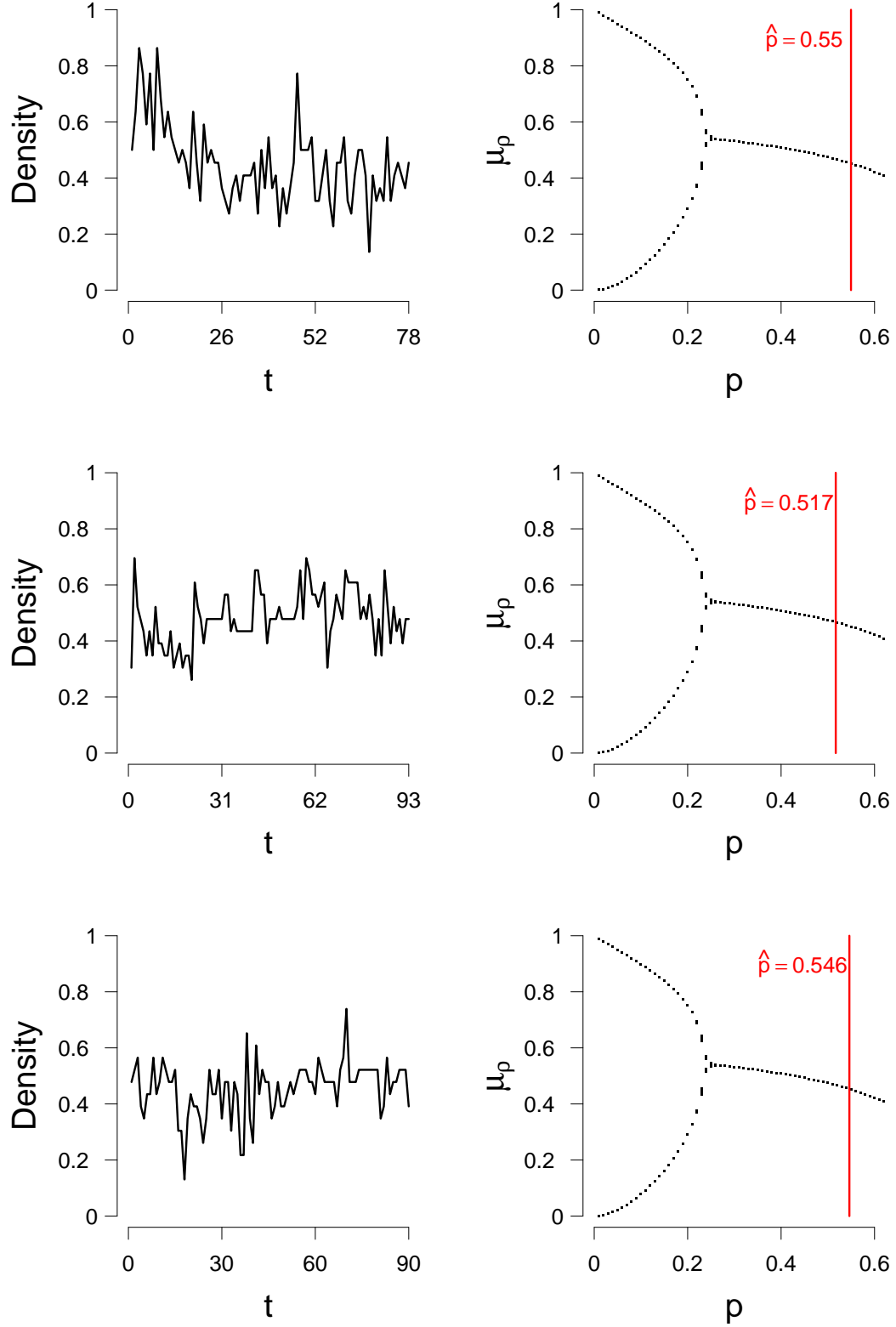


Figure 12: The evolution of the percentage of active nodes for each time point (left column), and the bifurcation diagram (right column). Upper row = participant from the low-group. Middle row = participant from the medium-group. Lower row = participant from the high-group. The red line in the bifurcation diagram indicates the estimate of p . μ_p = the expected density calculated with equation (4).

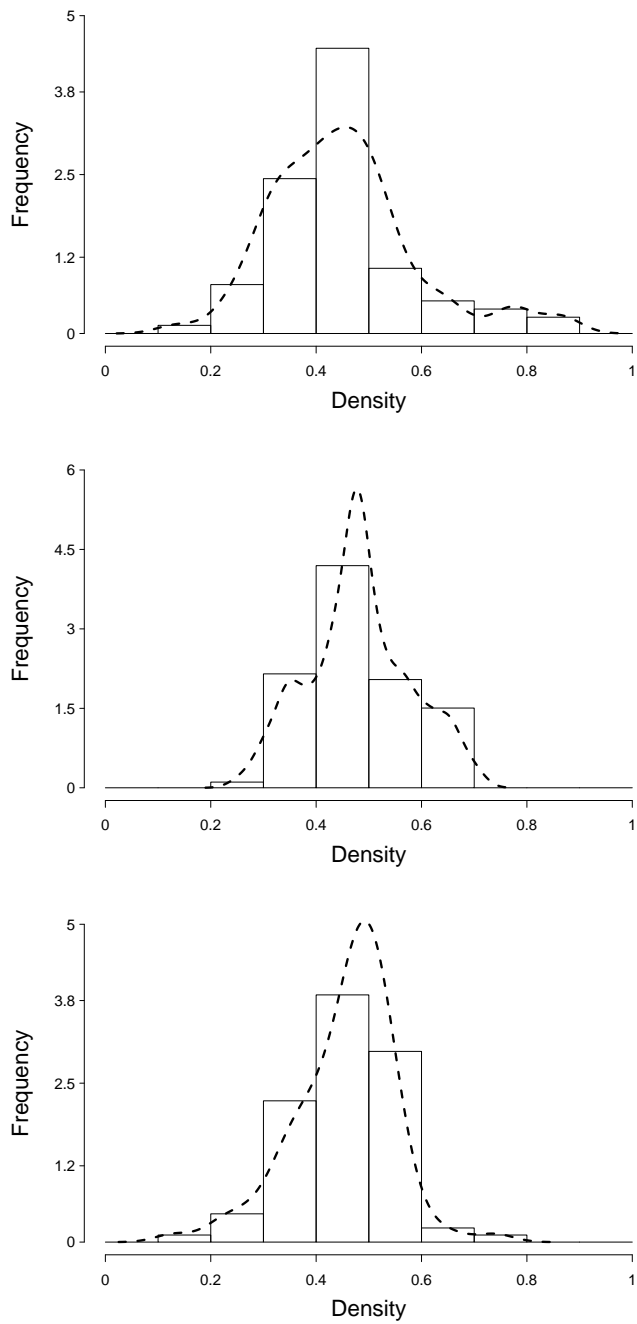


Figure 13: Distributions of the graph densities calculated at each time point for the three participants of the general sample. The dashed line represents the Kernel density of the distribution.